



**HAL**  
open science

## Unsteady rising of clean bubble in low viscosity liquid

José Manuel Gordillo, Benjamin Lalanne, Frederic Risso, Dominique Legendre, Sébastien Tanguy

► **To cite this version:**

José Manuel Gordillo, Benjamin Lalanne, Frederic Risso, Dominique Legendre, Sébastien Tanguy. Unsteady rising of clean bubble in low viscosity liquid. *Bubble Science, Engineering and Technology*, 2012, vol. 4, pp. 4-11. 10.1179/1758897912Y.0000000002 . hal-00920787

**HAL Id: hal-00920787**

**<https://hal.science/hal-00920787>**

Submitted on 19 Dec 2013

**HAL** is a multi-disciplinary open access archive for the deposit and dissemination of scientific research documents, whether they are published or not. The documents may come from teaching and research institutions in France or abroad, or from public or private research centers.

L'archive ouverte pluridisciplinaire **HAL**, est destinée au dépôt et à la diffusion de documents scientifiques de niveau recherche, publiés ou non, émanant des établissements d'enseignement et de recherche français ou étrangers, des laboratoires publics ou privés.



## Open Archive TOULOUSE Archive Ouverte (OATAO)

OATAO is an open access repository that collects the work of Toulouse researchers and makes it freely available over the web where possible.

This is an author-deposited version published in : <http://oatao.univ-toulouse.fr/>  
Eprints ID : 10560

**To link to this article** : DOI:10.1179/1758897912Y.0000000002  
URL : <http://dx.doi.org/10.1179/1758897912Y.0000000002>

**To cite this version** : Gordillo, José Manuel and Lalanne, Benjamin and Risso, Frederic and Legendre, Dominique and Tanguy, Sébastien Unsteady rising of clean bubble in low viscosity liquid. (2012) Bubble Science, Engineering and Technology, vol. 4 (n° 1). pp. 4-11. ISSN 1758-8960

Any correspondence concerning this service should be sent to the repository administrator: [staff-oatao@listes-diff.inp-toulouse.fr](mailto:staff-oatao@listes-diff.inp-toulouse.fr)

# Unsteady rising of clean bubble in low viscosity liquid

J. M. Gordillo\*<sup>1</sup>, B. Lalanne<sup>2</sup>, F. Risso<sup>2</sup>, D. Legendre<sup>2</sup> and S. Tanguy<sup>2</sup>

When a submerged bubble is initially at rest in a stagnant low viscosity liquid such as water, buoyancy forces accelerate the bubble upwards. The increasing relative velocity of the bubble with the surrounding liquid provokes deformations on the bubble shape that affect its vertical acceleration and also induce surface tension driven oscillations. Our theoretical model, which is compared with full Navier–Stokes simulations predicts, with a reasonable accuracy, both the position of the bubble centre of mass, as well as the time varying bubble shape under those conditions for which the Reynolds number is large, the amplitude of the deformation is small, the bubble interface is free of surfactants and the bubble rises following a straight vertical path. The model can be used as a first approximation to describe the initial instants of the unsteady buoyancy driven rising of millimetre sized bubbles typically generated in water aerators.

**Keywords:** Modelling, Numerical simulations

## Introduction

Oxygenation of a liquid is a basic process of chemical industry which, in practice, is achieved by injecting either air or pure oxygen through nozzles or pipes placed at the bottom of a stagnant liquid pool. Clearly, the mass transfer process from the bubble towards the liquid occurs in the interval of time comprised between the instant of generation and the one at which the bubble meets the free interface. Since the bubble shape at detachment is rather different from that it possesses when it reaches the terminal velocity, the transition from the shape at generation and the steady, final shape, takes place through a series of oscillations. These oscillations are associated with two facts:

- (i) the initial interfacial energy of the bubble is different from that it possesses when it reaches its terminal velocity
- (ii) since the acceleration associated to buoyancy forces increases the bubble relative velocity with the surrounding medium, the time varying pressure distribution along the bubble interface induces changes in the bubble shape in order to meet the dynamic boundary condition at the bubble surface. It is well known that the virtual mass of an object depends on its shape, so the surface tension driven oscillations of the bubble provoke unsteady accelerations of its centre of mass.

The purpose of this paper is to derive from first principles a model describing the interfacial oscillations as well as the associated unsteady acceleration of the bubble centre of mass that takes place during the gravity driven rising of bubbles initially at rest. The model is constructed under the following hypotheses: the local Reynolds number is large, the relative deformation of the bubble is small, the bubble rises following a vertical path and the bubble interface is clean, meaning that the shear stress at the bubble interface is zero. This latter assumption is the most restrictive one since, for it to be realistic, the liquid needs to be free of surfactants and this occurs only in those cases in which the liquid is either non-polar or water is ultrapurified.<sup>1</sup>

The same physical situation as the one considered here has constituted the subject of previous studies.<sup>2,3</sup> In those works, experiments were compared with the equations of motion obtained using force and energy balances. The system of equations derived in Refs. 2 and 3 requires a closing relationship related to the shape of the bubble, which is forced to be either the experimentally determined one or an ellipsoid. From a purely numerical point of view, Yang *et al.*<sup>4</sup> reported full Navier–Stokes simulations to reproduce the rise and distortion of bubbles rising into a liquid bath whose pressure could be arbitrarily varied in time.

Although, as it has been described above, the acceleration from the rest of deformable bubbles has received some attention in the literature, none of the previous studies report equations describing, in a self-consistent manner, the coupling between the bubble acceleration and its deformation. To fill in this gap, it is reported here that a theoretical approximation, assuming small deformations of the bubble around its unperturbed spherical shape, provides two differential equations to describe the unsteady rising of bubbles in a low viscosity liquid free of surfactants.

<sup>1</sup>Área de Mecánica de Fluidos, Departamento de Ingeniería Aeroespacial y Mecánica de Fluidos, Universidad de Sevilla, Avda. de los Descubrimientos s/n, 41092, Sevilla, Spain

<sup>2</sup>Institut de Mécanique des Fluides de Toulouse, CNRS, Université de Toulouse (INP, UPS), Allée Camille Soula, 31400 Toulouse, France

\*Corresponding author, email jgordill@us.es

## Theoretical description

The equations to be deduced next intend to model the unsteady vertical rising of millimetric air bubbles in pure water. Therefore, the typical values of the liquid density and liquid viscosity are  $\rho=10^3 \text{ kg m}^{-3}$  and  $\mu=10^{-3} \text{ Pa s}^{-1}$  respectively for a characteristic temperature of  $20^\circ\text{C}$ ; the corresponding values for the gas are, at the same temperature,  $\rho_g=1.2 \text{ kg m}^{-3}$  and  $\mu_g=1.810^{-5} \text{ Pa s}^{-1}$ . Since the typical velocity of the bubble is given by  $\sim O(gR)^{1/2}$ ,<sup>1</sup> with  $g$  and  $R$  denoting the gravitational acceleration and the unperturbed bubble radius respectively, the characteristic values of the Bond, Reynolds and Ohnesorge numbers for millimetric size bubbles [ $R \sim O(1) \text{ mm}$ ] rising in pure water are given by

$$\begin{aligned} \text{Bo} &= \frac{\rho g R^2}{\sigma} \sim 0.1 \\ \text{Oh} &= \frac{\mu}{(\rho\sigma R)^{1/2}} \sim 10^{-2} \\ \text{Re} &= \frac{\rho(gR)^{1/2}R}{\mu} = (\text{Bo})^{1/2}\text{Oh}^{-1} \sim 30 \end{aligned} \quad (1)$$

with  $\sigma=0.072 \text{ N m}^{-1}$  the interfacial coefficient of pure water at  $20^\circ\text{C}$ . The model assumes that the interface is free of surfactants and the viscosity contrast between the liquid and the gas is

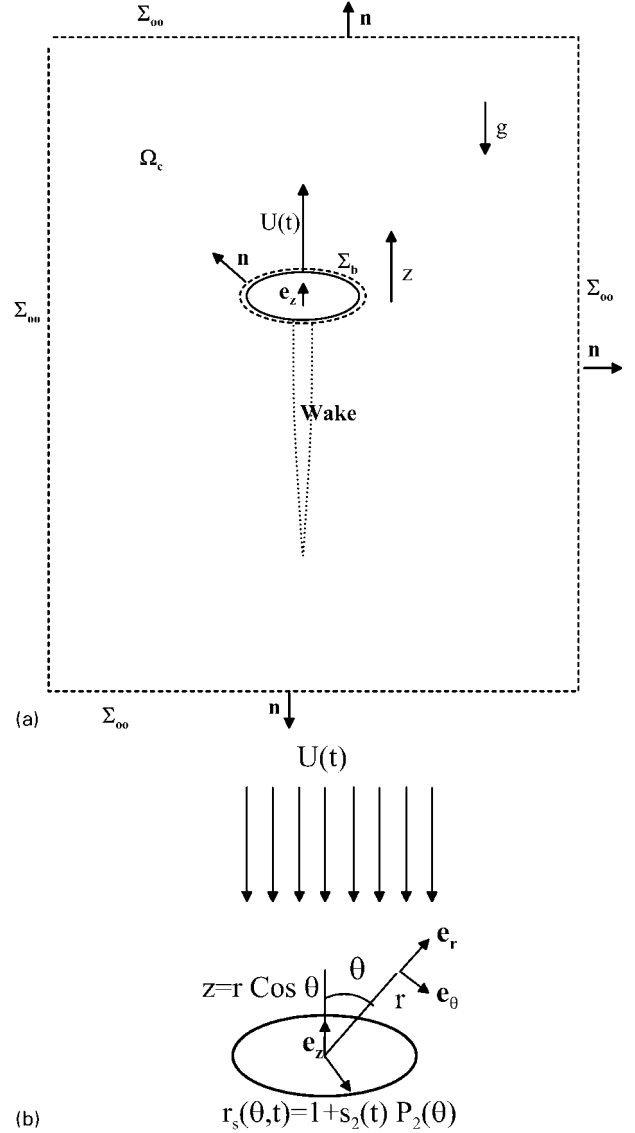
$$\mu_l/\mu_g \sim O(100)$$

consequently, the shear stress at the bubble interface is approximately zero.<sup>1</sup> Notice that the main consequence of considering a free slip boundary condition at the bubble interface is that, for the characteristic values of the dimensionless parameters given in equation (1), vorticity is confined to narrow regions, i.e. a boundary layer surrounding the bubble and a wake originated at its rear stagnation point extending downstream (see Fig. 1). Therefore, the flow is irrotational in the majority of the liquid bulk<sup>1</sup> and, thus, the velocity field in this large free vorticity region, can be expressed as a function of a potential  $\phi$ . Moreover, since the viscous wake at the rear part of rising bubbles with sizes  $R \lesssim 0.91 \text{ mm}$  is stable,<sup>1</sup> the model assumes that the bubble rises following a vertical path. It will also be assumed that the bubble is axisymmetric and that it is only slightly deformed around its initial spherical shape. Finally, the consequence of the large density contrast existing between the liquid and the air is that inertial effects in the gas are neglected and, consequently, pressure is uniform inside the bubble.

The purpose of this paper is to derive a reduced order model to predict the rising velocity of the bubble centre of mass  $U(t)$ , as well as the amplitude of the deformation  $s_2(t)$  (with  $t$  denoting time), under the starting hypotheses detailed above. In a frame of reference moving with the bubble dimensionless velocity  $U(t)$  (see Fig. 1), and using a system of spherical coordinates sketched in Fig. 1b, with the radial position  $r$ , the azimuthal angle  $\theta$  and the associated unit vectors  $\mathbf{e}_r$  and  $\mathbf{e}_\theta$ , the amplitude of the deformation  $s_2(t)$  is defined from the equation that approximately determines the position of the interface  $r_s(\theta, t)$  as follows

$$r_s = 1 + s_2(t)P_2(x) \quad (2)$$

where  $x=\cos \theta$  and  $P_i$  is the  $i$ th order Legendre polynomial [ $P_1=x$ ,  $P_2=(1/2)\times(3x^2-1)$ ]. Notice that



**1 a** sketch showing volume  $\Omega_c$  delimited by surfaces  $\Sigma_\infty$  and bubble interface  $\Sigma_b$ , where global balances of energy and vertical momentum are applied in order to deduce simplified equations of motion: bubble rises at dimensionless velocity  $U(t)$  and  $g$  denotes gravitational acceleration; unit vector  $\mathbf{e}_z$  points upwards, in direction opposite to gravity and coordinate  $z$  is vertical axis and **b** sketch showing system of spherical coordinates  $(r, \theta)$  with unit vectors  $\mathbf{e}_r$  and  $\mathbf{e}_\theta$  in frame of reference moving with bubble velocity  $U(t)$

equation (2) has been made dimensionless using the unperturbed bubble radius  $R$  and, also, that equation (2) can be expressed in the following way

$$S(r, t, \theta) = r_s - 1 - s_2(t)P_2(x) = 0. \quad (3)$$

The system of two equations needed to calculate the time evolution of the two dimensionless unknowns, namely,  $U(t)$  and  $s_2(t)$ , will be deduced applying global balances of vertical momentum and kinetic energy to the region  $\Omega_c$  delimited by the surfaces  $\Sigma_\infty$  and  $\Sigma_b$  depicted in Fig. 1a. It is important to notice that the boundary at infinity  $\Sigma_\infty$  does not intersect the growing wake formed at the rear part of the bubble and, thus, the Euler–Bernoulli equation can be used to relate the velocity potential with pressure in this region located very far

from the bubble interface. From now on all the variables are made dimensionless using the following scales: the vertical coordinate  $z$  (see Fig. 1) and the distance to the centre of the bubble  $r$  are made dimensionless using the unperturbed radius  $R$ , the velocity field  $\mathbf{u}$  as well as the rising velocity  $U$ , are made dimensionless using  $(gR)^{1/2}$ , the non-dimensional time  $t$  is made dimensionless using  $R/(gR)^{1/2}$ , the non-dimensional velocity potential  $\phi$  is made dimensionless using  $R(gR)^{1/2}$  and, finally, the scale used to obtain the non-dimensional values of the liquid pressure  $p$ , the gas pressure  $p_g$ , the capillary pressure

$$\text{Bo}^{-1}\nabla\cdot\mathbf{n} \quad (4)$$

where  $\mathbf{n}$  is the outer normal to the bubble surface shown in Fig. 1, as well as the viscous stress at the interface

$$2\text{Re}^{-1}\mathbf{n}\cdot\underline{\underline{\gamma}} \quad (5)$$

with

$$\underline{\underline{\gamma}} = 1/2[\nabla\mathbf{u} + (\nabla\mathbf{u})^T], \quad (6)$$

is  $\rho gR$

The first step to derive the two desired equations is to express the velocity potential  $\phi$ , as a function of the two unknowns, namely,  $U(t)$  and  $s_2(t)$ . Note first that the stress balance at the interface reads

$$-p\mathbf{n} + 2\text{Re}^{-1}\mathbf{n}\cdot\underline{\underline{\gamma}} + \mathbf{n}p_g - \text{Bo}^{-1}\mathbf{n}\nabla\cdot\mathbf{n} = 0, \quad (7)$$

i.e. tangential stress is zero at the interface of the bubble. This fact implies, as pointed out above, that vorticity is confined to narrow regions:<sup>1</sup> a boundary layer surrounding the bubble and a wake originated at its rear stagnation point that extends downstream. This suggests to express the liquid velocity field as  $\mathbf{u} = \nabla\phi + \Delta\mathbf{u}$ , with  $\Delta\mathbf{u} \neq 0$  only in the aforementioned narrow rotational regions of the flow. Moreover, since the bubble volume is constant, the potential  $\phi$  can be expressed as an expansion in spherical harmonics of the form

$$\phi \simeq \frac{a_1(t)}{r^2}P_1(x) + \frac{a_2(t)}{r^3}P_2(x) \quad (8)$$

where only the first two terms in the spherical harmonics expansion of the potential have been retained. The relationship between the unknown functions  $a_1$  and  $a_2$  in equation (8) with the two unknowns, is found by means of the kinematic boundary condition

$$\frac{\partial S}{\partial t} + \{-U\mathbf{e}_z + \nabla\phi[r=r_s(\theta,t)]\} \cdot \nabla S = 0 \quad (9)$$

with the function  $S$  defined in equation (3) and  $\mathbf{e}_z$  the unitary vector pointing upwards depicted in Fig. 1. Indeed, using the equations for the potential  $\phi$  (equation (8)) and  $S$  (equation (3)) one obtains

$$\begin{aligned} \nabla\phi &= \frac{-2a_1}{r^3}P_1\mathbf{e}_r - \frac{a_1}{r^3}\sin\theta\mathbf{e}_\theta - \frac{3a_2}{r^4}P_2\mathbf{e}_r - \frac{a_2}{r^4}\sin\theta P_2'\mathbf{e}_\theta \\ \frac{\partial S}{\partial t} &= -\dot{s}_2P_2 \end{aligned} \quad (10)$$

$$\nabla S = \mathbf{e}_r + s_2P_2'\sin\theta\mathbf{e}_\theta$$

with primes denoting derivatives with respect to  $x$  and dots denoting time derivatives. Once equation (10) is particularised at  $r_s = 1 + s_2P_2(x)$ , substituted into equation (9) and the resulting expression is linearized using

$s_2 \ll 1$ , the following equation relating  $a_i$  ( $i=1, 2$ ) with  $s_2$  and  $U$  is obtained

$$\begin{aligned} -\dot{s}_2P_2 - U\cos\theta + UP_2'\sin^2\theta s_2 - 2a_1P_1 + \\ 6a_1P_1P_2s_2 - 3a_2P_2 + 12a_2P_2^2s_2 - \\ -a_1s_2P_2'\sin^2\theta + 3a_2s_2(P_2')^2\sin^2\theta = 0. \end{aligned} \quad (11)$$

By virtue of the orthogonality of Legendre polynomials with respect to the weight function  $\sin\theta$ , i.e.

$$\int_0^\pi P_n(\cos\theta)P_m(\cos\theta)\sin\theta d\theta = 0 \quad \text{for } n \neq m, \quad (12)$$

the following equations for  $a_i$

$$\begin{aligned} a_1 &= -\frac{U}{2}\left(1 - \frac{3}{5}s_2\right), \\ a_2 &= -\frac{\dot{s}_2}{3}, \end{aligned} \quad (13)$$

have been deduced once equation (11) is multiplied by  $P_1\sin\theta$  and is integrated between 0 and  $\pi$ . Now, substituting equation (13) into equation (8), the expression obtained for the potential  $\phi$  as a function of both  $U$  and  $s_2$  in the laboratory frame of reference reads,

$$\phi = -\frac{U}{2r^2}\left(1 - \frac{3s_2}{5}\right)P_1(x) - \frac{\dot{s}_2}{3r^3}P_2(x). \quad (14)$$

Once the potential  $\phi$  has been expressed as a function of the two unknowns, the equations for the time evolution of both the rising velocity  $U(t)$  and the deformation  $s_2(t)$  are obtained by means of the global balances of vertical momentum and kinetic energy applied to the control volume  $\Omega_c$  in Fig. 1. It is crucial to note that the global balances are referred to a laboratory frame of reference. Therefore, the two integral equations, which need to be solved subject to the dynamic boundary condition at the free interface (equation (7)) and to the kinematic condition

$$\mathbf{u}\cdot\mathbf{n} = \nabla\phi\cdot\mathbf{n}, \quad (15)$$

$$\Delta\mathbf{u}\cdot\mathbf{n} = 0,$$

read, respectively,

$$\begin{aligned} \mathbf{e}_z \cdot \left[ \frac{d}{dt} \int_{\Omega_c} (\nabla\phi + \Delta\mathbf{u}) d\omega = \int_{\Sigma_b} (p\mathbf{n} - 2\text{Re}^{-1}\mathbf{n}\cdot\underline{\underline{\gamma}}) d\sigma + \right. \\ \left. \int_{\Omega_c} -\mathbf{e}_z d\sigma - \int_{\Sigma_\infty} (\mathbf{n}p + \mathbf{n}\cdot\mathbf{u}\mathbf{u}) d\sigma \right] \end{aligned} \quad (16)$$

and

$$\begin{aligned} \frac{1}{2} \frac{d}{dt} \int_{\Omega_c} (\nabla\phi\cdot\nabla\phi + 2\nabla\phi\cdot\Delta\mathbf{u} + |\Delta\mathbf{u}|^2) d\omega = \\ \int_{\Sigma_b} \mathbf{u}\cdot(p\mathbf{n} - 2\text{Re}^{-1}\mathbf{n}\cdot\underline{\underline{\gamma}}) d\sigma - \int_{\Omega_c} \end{aligned} \quad (17)$$

$$\mathbf{e}_z\cdot\mathbf{u}d\sigma - 2\text{Re}^{-1} \int_{\Omega_c} \underline{\underline{\gamma}} : \underline{\underline{\gamma}} d\omega - \int_{\Sigma_\infty} \mathbf{u}\cdot\mathbf{n} \left( p + \frac{|\mathbf{u}|^2}{2} \right) d\sigma.$$

Since

$$-\mathbf{e}_z = -\nabla z \quad (18)$$

and due to the fact that the liquid is incompressible ( $\nabla\cdot\mathbf{u}=0$ ,  $\nabla\cdot\Delta\mathbf{u}=0$ ), which implies that

$$-\mathbf{e}_z\cdot\mathbf{u} = -\nabla\cdot(\mathbf{z}\mathbf{u}) \quad (19)$$

$$\nabla^2 \phi = 0 \quad (20)$$

$$\nabla \cdot (\phi \nabla \phi) = \nabla \phi \cdot \nabla \phi \quad (21)$$

$$\nabla \cdot (\Delta \mathbf{u} \phi) = \nabla \phi \cdot \Delta \mathbf{u} \quad (22)$$

the volume integrals in the equations (16) and (17) can be transformed to surface integrals using equations (18)–(22) by means of the Gauss integral theorem.

Using the boundary conditions (7), (15) as well as equations (18)–(22), equation (16) can be expressed as

$$\mathbf{e}_z \cdot \left( \frac{d}{dt} \int_{\Sigma_b} -\phi \mathbf{n} d\sigma = \int_{\Sigma_b} z \mathbf{n} d\sigma - \frac{d}{dt} \int_{\Omega_c} \Delta \mathbf{u} d\omega \right) \quad (23)$$

where it has been taken into account the additional fact that the net force on the bubble is zero, i.e

$$\int_{\Sigma_b} (-p \mathbf{e}_z \mathbf{n} + \text{Bo}^{-1} \nabla \cdot \mathbf{n}) d\sigma = 0. \quad (24)$$

The use of equations (7), (15) and (18)–(22) also leads to the following expression for the kinetic energy equation (17)

$$\begin{aligned} \frac{1}{2} \frac{d}{dt} \int_{\Sigma_b} -\phi \nabla \phi \cdot \mathbf{n} d\sigma &= -\text{Bo}^{-1} \int_{\Sigma_b} \nabla \cdot \mathbf{n} \nabla \phi \cdot \mathbf{n} d\sigma + \int_{\Sigma_b} z \nabla \phi \cdot \mathbf{n} d\sigma - \\ &- 2\text{Re}^{-1} \int_{\Omega_c} \underline{\underline{\gamma}} : \underline{\underline{\gamma}} d\omega - \int_{\Omega_c} \frac{|\Delta \mathbf{u}|^2}{2} d\omega \end{aligned} \quad (25)$$

Let us point out that to deduce equations (23)–(25) it has been taken into account two additional facts: first, since  $\phi \rightarrow r^{-2}$  and  $\nabla \phi \rightarrow r^{-3}$  for  $|\mathbf{r}| \rightarrow \infty$ , the integral

$$\int_{\Sigma_\infty} \phi \nabla \phi \cdot \mathbf{n} d\sigma \rightarrow 0 \quad (26)$$

and, second, due to the fact that the wake does not cross the outer boundary,  $\Delta \mathbf{u} = 0$  at  $\Sigma_\infty$  and, since  $\mathbf{u} = \nabla \phi + \Delta \mathbf{u}$

$$p + \partial \phi / \partial t + |\mathbf{u}|^2 / 2 + z = p + \partial \phi / \partial t + |\nabla \phi|^2 / 2 + z = C(t) \quad (27)$$

at  $\Sigma_\infty$  by virtue of the Euler–Bernoulli equation.<sup>5</sup>

Now, it only remains to calculate each of the integrals appearing in equations (23) and (25). For that purpose note first that, retaining only linear terms in  $s_2$ , the unitary normal vector to the interface  $\Sigma_b$  can be approximated as

$$\mathbf{n} \simeq \mathbf{e}_r + s_2 \sin \theta P'_2 \mathbf{e}_\theta, \quad (28)$$

from which it follows that

$$\mathbf{n} \cdot \mathbf{e}_z \simeq \cos \theta - s_2 P'_2 \sin^2 \theta. \quad (29)$$

Also, retaining only linear terms in  $s_2$ , the differential surface element  $d\sigma$  in the surface integrals of equations (23) and (25) can be approximated as follows

$$d\sigma \simeq 2\pi \sin \theta (1 + 2s_2 P_2) d\theta. \quad (30)$$

Using the expression of the potential  $\phi$  given by equation (14), together with the results given in the set of equations (28)–(30), the integrals at the left of equations (23) and (25) read respectively

$$\mathbf{e}_z \cdot \frac{d}{dt} \int_{\Sigma_b} -\phi \mathbf{n} d\sigma \simeq \frac{2\pi}{3} \frac{d}{dt} \left( U - \frac{9}{5} U s_2 \right) \quad (31)$$

$$\frac{1}{2} \frac{d}{dt} \int_{\Sigma_b} -\phi \nabla \phi \cdot \mathbf{n} d\sigma \simeq \frac{4\pi}{15} \left\{ \dot{s}_2 \ddot{s}_2 + \frac{5}{4} \frac{d}{dt} \left[ U^2 \left( 1 - \frac{9}{5} s_2 \right) \right] \right\}, \quad (32)$$

where higher order terms in  $s_2$  have been neglected. Moreover, notice that the interfacial curvature of the bubble surface

$$\mathbf{n} = \frac{\nabla S}{|\nabla S|}, \quad (33)$$

can be approximated, retaining only linear terms in  $s_2$ , as

$$\nabla \mathbf{n} = 2 + 4P_2 s_2 - 10P_2^2 s_2^2 \simeq 2 + 4P_2 s_2 \quad (34)$$

Consequently, the power required to deform the bubble surface, represented by the first term at the right of equation (25), is given by

$$-\text{Bo}^{-1} \int_{\Sigma_b} \nabla \cdot \mathbf{n} \nabla \phi \cdot \mathbf{n} d\sigma = -\frac{16\pi}{5} \text{Bo}^{-1} \dot{s}_2 s_2. \quad (35)$$

The calculation of the integrals associated to the effect of gravitational forces (first and second terms at the right of equations (23) and (25) respectively) leads to the following results

$$\int_{\Sigma_b} z \mathbf{e}_z \cdot \mathbf{n} d\sigma = \frac{4\pi}{3}, \quad (36)$$

$$\int_{\Sigma_b} z \nabla \phi \cdot \mathbf{n} d\sigma = \frac{4\pi}{3} U, \quad (37)$$

where it has been taken into account that  $z(r_s, \theta) = (1 + s_2 P_2) \cos \theta$  and have made use of the equation for  $\phi$  (equation (14)). Finally, the power dissipated by viscous stresses (third integral at the right of equation (25)), namely

$$-2\text{Re}^{-1} \int_{\Omega} \underline{\underline{\gamma}} : \underline{\underline{\gamma}} d\omega, \quad (38)$$

can be easily calculated in the limit of high Reynolds numbers. Indeed, in those cases for which the Reynolds number is sufficiently large, the main contribution to the integral in equation (38) comes from the potential flow region.<sup>6</sup> In such cases, this integral can be calculated following Batchelor<sup>5</sup> as

$$\int_0^\pi \mathbf{n} \cdot \nabla (\nabla \phi \cdot \nabla \phi) 2\pi (1 + 2s_2 P_2) \sin \theta d\theta \quad (39)$$

The integrand in equation (39) divided by  $2\pi$  can be expressed as

$$\begin{aligned} (1 + 2s_2 P_2) \mathbf{n} \cdot \nabla (\nabla \phi \cdot \nabla \phi)|_{r=r_s} &\simeq -6 [(\dot{s}_2)^2 P_2^2 + 2U \dot{s}_2 P_2 \cos \theta] - \\ &- \frac{3}{2} \left[ \frac{4}{9} (\dot{s}_2)^2 (P'_2)^2 \sin^2 \theta + \frac{4}{3} U \dot{s}_2 \sin^2 \theta P'_2 \right] - 2\dot{s}_2 U P_2 \cos \theta - \\ &2(\dot{s}_2)^2 P_2^2 - \frac{1}{3} U \dot{s}_2 P'_2 \sin^2 \theta - \frac{2}{9} (\dot{s}_2)^2 (P'_2)^2 \sin^2 \theta - 6U^2 \cos^2 \theta - \\ &\frac{3}{2} U^2 \sin^2 \theta + 42U^2 s_2 P_2 \cos^2 \theta + \frac{36}{5} U^2 s_2 \cos^2 \theta + \\ &\frac{21}{2} U^2 s_2 P_2 \sin^2 \theta + \frac{18}{10} U^2 s_2 \sin^2 \theta - \frac{3}{2} U^2 s_2 P'_2 \sin^2 \theta \cos \theta - \\ &12U^2 s_2 P_2 \cos^2 \theta - 3U^2 s_2 P_2 \sin^2 \theta. \end{aligned} \quad (40)$$

and, therefore, the power dissipated by viscous stresses is approximately given, in the limit  $\text{Re} \gg 1$ , substituting equation (40) into equation (38)

$$\begin{aligned}
& -2\text{Re}^{-1} \int_{\Omega} \underline{\underline{\gamma}} : \underline{\underline{\gamma}} d\omega = \\
& -12\text{Re}^{-1} \pi U^2 (1 - 2s_2) - \frac{32\pi}{3} \text{Re}^{-1} s_2^2. \quad (41)
\end{aligned}$$

Consequently, the substitution of equations (31), (32), (35)–(37) and (41) into equations (23)–(25), leads to the following expressions for the vertical momentum and kinetic energy equations

$$\frac{2\pi}{3} \frac{d}{dt} \left( U - \frac{9}{5} s_2 U \right) = \frac{4\pi}{3} + F_v \quad (42)$$

with

$$F_v = - \frac{d}{dt} \int_{\Omega_c} \mathbf{e}_z \cdot \Delta \mathbf{u} d\omega \quad (43)$$

and

$$\begin{aligned}
& \frac{4\pi}{15} \frac{d}{dt} \left\{ \frac{s_2^2}{2} + \frac{5}{4} \left[ U^2 \left( 1 - \frac{9}{5} s_2 \right) \right] + 6\text{Bo}^{-1} s_2^2 \right\} = \\
& \frac{4\pi}{3} U - \frac{1}{\text{Re}} \left[ 12\pi U^2 (1 - 2s_2) + \frac{32\pi}{3} s_2^2 \right]. \quad (44)
\end{aligned}$$

Subtracting from equation (44) the result of multiplying equation (42) by  $U$ , the following couple of equations for both  $U$  and  $s_2$  is obtained

$$\frac{d}{dt} \left( U - \frac{9}{5} s_2 U \right) = 2 - 18U\text{Re}^{-1} (1 - 2s_2), \quad (45)$$

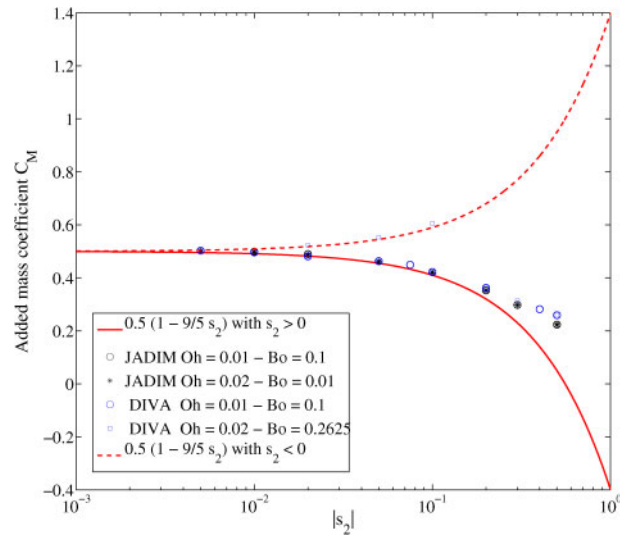
and

$$\frac{d^2 s_2}{dt^2} + 40\text{Re}^{-1} \frac{ds_2}{dt} + 12\text{Bo}^{-1} s_2 = - \frac{9}{4} U^2. \quad (46)$$

To deduce equations (45) and (46),  $F_v$  is not calculated, but identified with those terms proportional to  $U\text{Re}^{-1}$ . The kinetic energy contained in the regions where vorticity is different from zero (fourth integral at the right of equation (25)) has also been neglected. It will be discussed below that the system (45) and (46) is quite similar, albeit not identical, to that obtained by Doinikov,<sup>12</sup> who deduced his result by means of a different mathematical technique. Also notice that the terms representing both the natural oscillation frequency ( $12\text{Bo}^{-1}$ )<sup>1/2</sup> in equation (46) as well as the damping coefficient ( $40\text{Re}^{-1}$ ) in the same equation, coincide with the values for a bubble at rest<sup>13</sup> in spite of the bubble's centre of mass velocity is different from zero.<sup>14</sup>

## Results

The results of the model are compared with direct numerical simulations performed with two different codes solving the full Navier–Stokes equations but based on two different methods for the interface capture. In DIVA,<sup>7,8</sup> a level set ghost fluid method is used while in JADIM<sup>9–11</sup> a volume of fluid method with no interface reconstruction is implemented. The first check of the theory is depicted in Fig. 2, where the theoretical dimensionless added mass coefficient namely  $C_M = 1/2(1 - 9/5s_2)$  is compared with the one calculated with each of the numerical codes. The theoretical result, which has been deduced neglecting higher order terms in  $s_2$ , agrees well with numerical results for the smallest values of  $s_2$  but, as expected, the agreement deteriorates for  $s_2 \gtrsim 0.2$ .

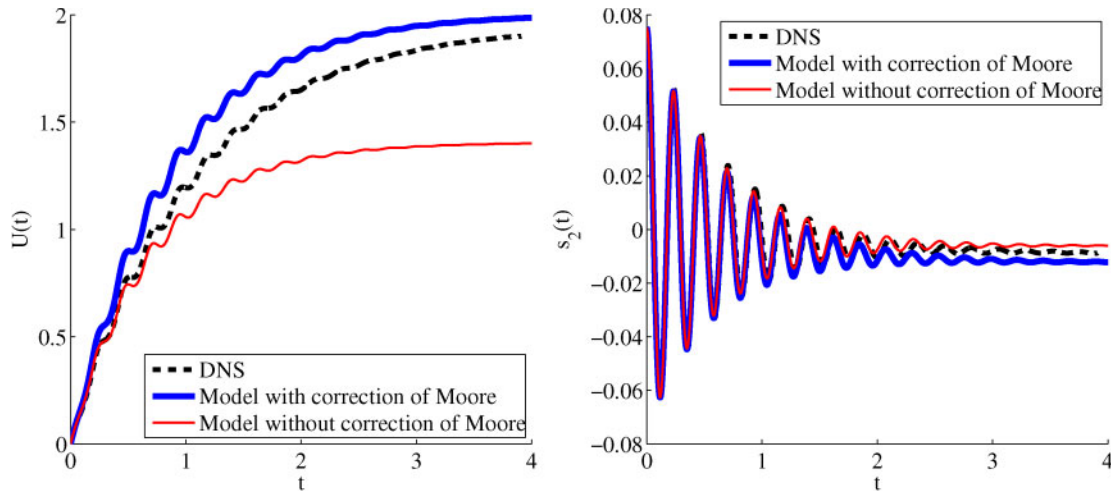


**2 Comparison between dimensionless added mass coefficient deduced in model  $1/2(1 - 9/5s_2)$  and the ones computed numerically using DIVA<sup>7,8</sup> or JADIM<sup>9–11</sup> codes for several values of Bond and Ohnesorge numbers defined in equation (1)**

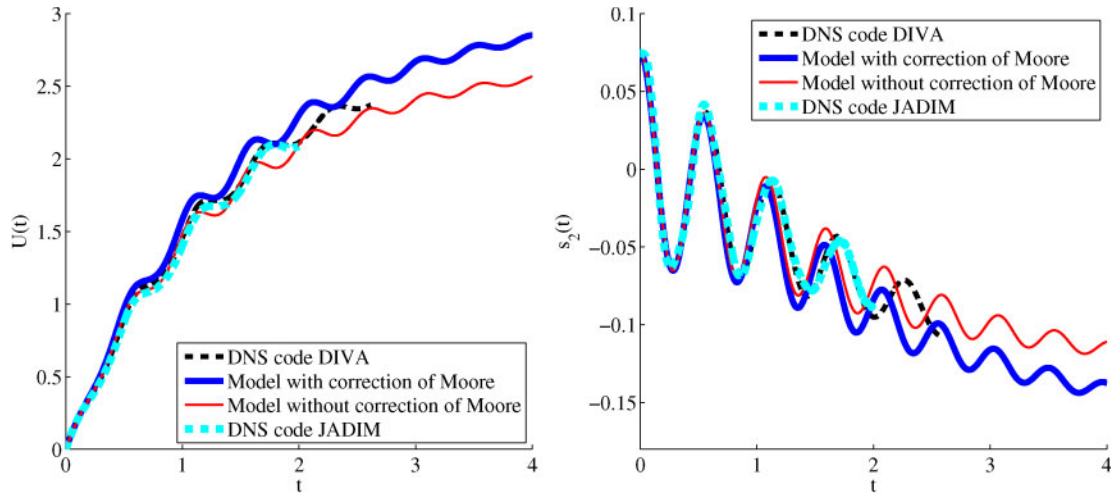
In Figs. 3–5, the time evolutions of both  $U(t)$  and  $s_2(t)$  predicted by equations (45) and (46) are compared with the ones computed numerically for several values of  $Bo$  and a fixed value of the Ohnesorge number

$$\text{Oh} = (\text{Bo})^{1/2} / \text{Re} = 0.01.$$

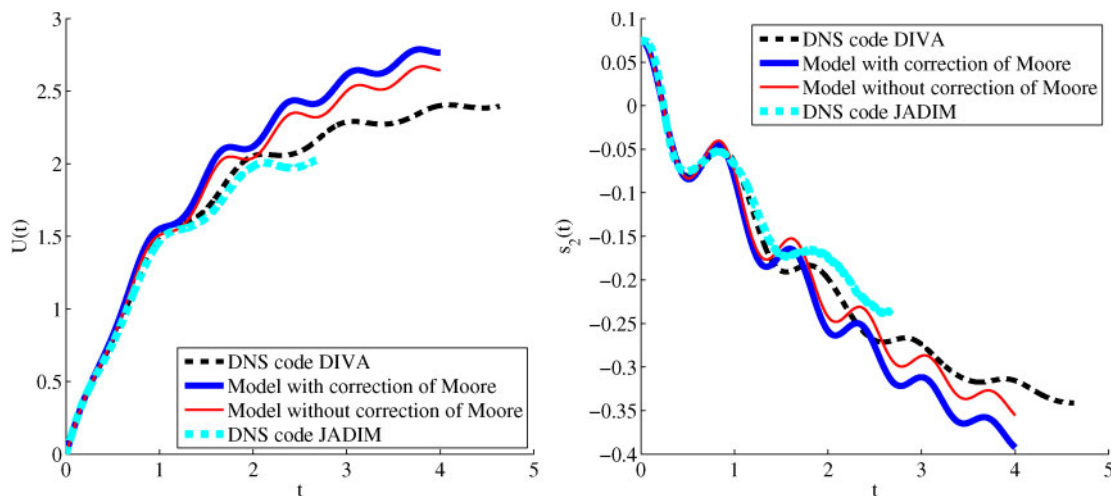
In the case of the smallest  $Bo$  considered,  $Bo = 0.0164$ , Fig. 3 shows that the time evolution of the bubble deformation is very well captured by the model. However, the ascending velocity is only reproduced during the initial instants of the acceleration process. There are two reasons that explain the mismatch between the time evolution of the centre of mass velocity  $U(t)$ , predicted by the set of equations (45) and (46) and the numerical result. One of them is that the theory developed here only retains linear terms in  $s_2$ . However, the main reason for the disagreement between theory and numerics depicted in Figs. 3–5 is associated to the fact that the theoretical results deduced here are only valid in the limit  $\text{Re} \gg 1$ . Indeed, the fourth integral on the right hand side of equation (25) has been neglected, so the viscous dissipation that takes place into both the unsteady boundary layer and the unsteady wake is not taken into account by the model. The calculation of the dissipation in these regions where vorticity is confined, would lead to a generalised memory force term in equations (45) and (46) that would clearly improve the results, but the correct quantification of this new term is out of the scope of this study. Nevertheless, it can be checked whether the addition to the term proportional to  $\text{Re}^{-1}$  in equation (45) of the  $\sim O(\text{Re}^{-3/2})$  viscous correction term due to Moore,<sup>6</sup> improves the comparison between theory and numerical results or not. Notice, however, that the origin of Moore's correction<sup>6</sup> corresponds to the viscous dissipation taking place into both the boundary layer and the wake of a bubble moving steadily. In spite that the type of flow in the physical situation studied here is unsteady, if the term proportional to  $\text{Re}^{-1}$  in equation (45) is substituted by Moore's result, i.e.



3 Theoretical time evolution of vertical velocity  $U(t)$  and bubble distortion  $s_2(t)$  compared with numerical results for  $Bo=0.0164$  and  $Oh=Bo^{1/2}/Re=0.01$ : results of model have been calculated including and not including Moore's correction term, whereas numerical simulation has been performed using DIVA;<sup>7,8</sup> in this case, addition of viscous term by Moore,<sup>6</sup> improves prediction of terminal velocity; results corresponding to JADIM<sup>9-11</sup> code have not been included since magnitude of numerical spurious currents is important when compared to velocity of bubble



4 Theoretical time evolution of vertical velocity  $U(t)$  and bubble distortion  $s_2(t)$  compared with numerical results for  $Bo=0.0945$  and  $Oh=Bo^{1/2}/Re=0.01$ : results of model have been calculated including and not including Moore's correction term, whereas numerical simulation has been performed using either DIVA<sup>7,8</sup> or JADIM<sup>9-11</sup> numerical codes; agreement between theory and numerics is not only fairly good during initial stages of acceleration process, but also at intermediate times



5 Theoretical time evolution of vertical velocity  $U(t)$  and bubble distortion  $s_2(t)$  compared with numerical results for  $Bo=0.2625$  and  $Oh=Bo^{1/2}/Re=0.01$ : results of model have been calculated including and not including Moore's correction term, whereas numerical simulation has been performed using either DIVA<sup>7,8</sup> or JADIM<sup>9-11</sup> numerical codes; For this large value of Bond number, amplitude of bubble deformation  $s_2(t)$  for large times, invalidates initial assumption of  $s_2 \ll 1$

$$18 U \text{Re}^{-1}(1-2s_2) \times \left[1-2\cdot 2/(2\text{Re}U)^{1/2}\right]$$

the agreement with numerical results notably improves in the case depicted in Fig. 3. Indeed, notice that the terminal velocity predicted by the model is closer to the numerical result than that in the case of the  $\sim O(\text{Re}^{-3/2})$  term  $[-2\cdot 2/(2\text{Re}U)^{1/2}]$  is neglected.

The fact that the equations (45) and (46) have been deduced retaining only linear terms in  $s_2$ , also poses limitations to the theory. This is clearly seen in Fig. 5, where the results corresponding to the larger value of  $Bo$  are depicted: since the bubble deformation  $s_2$  increases with  $Bo$ , the agreement depicted in Fig. 5 between theory and the numerics, is the poorest of the three cases considered. Notice also that the agreement between the numerics and theory in the case depicted in Fig. 4, which corresponds to the case of bubbles with  $R \simeq 1$  mm, is reasonable for all times. This is due to the fact that the starting hypotheses with which the present model has been deduced correspond, precisely, to this bubble size.

Let us conclude stating that the agreement between theory and numerics is fairly good during the initial stages of the acceleration process with independence of the value of  $Bo$  considered. However, the good agreement deteriorates for larger times due to the fact that the model does not appropriately account for the viscous dissipation in the narrow time varying regions where vorticity is confined, namely, the boundary layer and the wake.

## Conclusions

This paper presents a model that can be used as a first approximation to describe the initial instants of the unsteady buoyancy driven rising of millimetre sized bubbles generated in water aerators. More precisely, the authors have deduced an approximate theoretical model which includes two equations to describe the time evolutions of both the vertical velocity and the distortions experienced by a clean bubble which accelerates from the rest due to the action of buoyancy forces. The theoretical analysis developed here assumes that the bubble deformation is small and that the Reynolds number is sufficiently large so as to neglect the dissipation in both the unsteady boundary layer and the wake. The main contribution of this paper is that the reduced order model deduced retains, in a self-consistent manner, the effects on the virtual mass of the bubble of the distortions created by the increasing relative velocity of the bubble with the surrounding liquid and by capillary oscillations. In addition, the terms associated with viscosity are correctly calculated up to first order in the limit of high Reynolds numbers and small deformations. The main differences of the theory developed here with the ones presented previously are the following. Differently to van Wijngaarden and Veldhuis<sup>2</sup> it is not assumed here that the bubble is ellipsoidal, viscosity is retained in the present analysis up to first order and the effect of the bubble centre of mass velocity on the bubble oscillations is also taken into account. In the paper by de Vries and Lohse,<sup>3</sup> the bubble is also assumed to be ellipsoidal but, differently to the theoretical approach by van Wijngaarden and Veldhuis,<sup>2</sup> both the viscous drag and the effect of the bubble velocity on its shape, are retained in their model. However, the theory by de Vries

and Lohse<sup>3</sup> needs to be fed with the experimentally measured aspect ratio of the bubbles. In Yang *et al.*,<sup>4</sup> the authors simplified the analysis considering that the rising bubble is spherical. Their model retained the effect of the history force through a term which is only valid for the case of spherical bubbles moving at low Reynolds numbers. In spite of the addition of such term is not justified in the range of Reynolds numbers considered in their study, Yang *et al.*<sup>4</sup> found that its inclusion improves the comparison with direct numerical simulations. Finally, Doinikov<sup>12</sup> deduced, in a self-consistent manner but neglecting viscosity, a system of equations for both the vertical position of the bubble centre of mass and the shape oscillations retaining four terms in the expansion of the potential  $\phi$  in spherical harmonics. Following a different mathematical technique, the author found a system of ordinary differential equations very similar to that deduced here. However, in Doinikov's paper,<sup>12</sup> viscous terms are included *ad hoc* and only in the equation that represents the vertical rising velocity (equation (45) for  $U(t)$  here). In addition, the viscous term added *ad hoc* by Doinikov assumes that the bubble is spherical. This is not consistent with the potential flow part of the analysis, where it is considered that the bubble is deformable.

The comparison with full Navier Stokes simulations using two different numerical codes reveal that with independence of the  $Bo$  number, the agreement between theory and numerics is fairly good during the initial instants of time. However, the good agreement deteriorates for larger values of the dimensionless time. This indicates that the inertia of the liquid contained in the viscous regions, which would appear in equations (45) and (46) in the form of a generalised history force of the type included in their model by Yang *et al.*<sup>4</sup> cannot be neglected in the analysis. An alternative to account for the viscous dissipation in the regions where vorticity is confined, would be to follow the procedure in Legendre *et al.*,<sup>15</sup> where the history force term is calculated numerically. The other possibility would be to follow an analytical approach. This latter option implies to describe the time evolution of the vorticity in the narrow regions where it is confined. This would lead to a set of boundary layer equations for the flow around the bubble and the wake, a non-trivial calculation which is out of the scope of this preliminary study.

## Acknowledgements

J. M. Gordillo thanks financial support by the Spanish Ministry of Education under project DPI2011-28356-C03-01 and the Junta de Andalucía under project P08-TEP-03997.

## References

1. J. Magnaudet and I. Eames: 'The motion of high Reynolds number bubbles in inhomogeneous flows', *Ann. Rev. Fluid Mech.*, 2000, **32**, 659–708.
2. L. van Wijngaarden and C. Veldhuis: 'On hydrodynamical properties of ellipsoidal bubbles', *Acta Mech.*, 2008, **201**, 37–46.
3. J. de Vries and D. Lohse: 'Induced bubble shape oscillations and their impact on the rise velocity', *Eur. Phys. J. B*, 2002, **29B**, 503–509.
4. B. Yang, A. Prosperetti and S. Takagi: 'The transient rise of a bubble subject to shape or volume changes', *Phys. Fluids*, 2003, **15**, 2640–2648.
5. G. K. Batchelor: 'An introduction to fluid dynamics'; 2000, Cambridge, Cambridge University Press.

6. D. W. Moore: 'The boundary layer on a spherical gas bubble', *J. Fluid Mech.*, 1963, **16**, 161–176.
7. S. Tanguy and A. Berlemont: 'Application of a level set method for simulation of droplet collisions', *Int. J. Multiph. Flow*, 2005, **31**, 1015–1035.
8. S. Tanguy, T. Menard and A. Berlemont: 'A level set method for vaporizing two-phase flows', *J. Comput. Phys.*, 2007, **221**, 837–853.
9. T. Bonometti and J. Magnaudet: 'An interface capturing method for incompressible two-phase flows: validation and application to bubble dynamics', *Int. J. Multiph. Flow*, 2007, **33**, (2), 109–133.
10. J.-B. Dupont and D. Legendre: 'Numerical simulation of static and sliding drop with contact angle hysteresis', *J. Comput. Phys.*, 2010, **229**, 2453–2478.
11. T. Abadie, J. Aubin, D. Legendre and C. Xuereb: 'Hydrodynamics of gas-liquid Taylor flow in rectangular microchannels', *Microfluid. Nanofluid.*, 2012, **12**, 355–369.
12. A. A. Doinikov: 'Translational motion of a bubble undergoing shape oscillations', *J. Fluid Mech.*, 2004, **501**, 1–24.
13. A. Prosperetti: 'Free oscillations of drops and bubbles: the initial-value problem', *J. Fluid Mech.*, 1980, **100**, 333–347.
14. S. V. Subramanyam: 'A note on the damping and oscillations of a fluid drop moving in another fluid', *J. Fluid Mech.*, 1969, **37**, 715–725.
15. D. Legendre, J. Borée and J. Magnaudet: 'Thermal and dynamic evolution of a spherical bubble moving steadily in a superheated or subcooled liquid', *Phys. Fluids*, 1998, **10**, 1256–1272.